

X-ray absorption spectroscopy and X-ray magnetic
circular dichroism studies of transition-metal-co-doped
ZnO nano-particles

T. Kataoka, Y. Yamazaki, V. R. Singh, Y. Sakamoto, K. Ishigami,
V. K. Verma, and A. Fujimori

*Department of Physics and Department of Complexity Science and
Engineering, University of Tokyo, Bunkyo-ku, Tokyo 113-0033, Japan*

F.-H. Chang, H.-J. Lin, D. J. Huang, and C. T. Chen

National Synchrotron Radiation Research Center, Hsinchu 30076, Taiwan

D. Asakura and T. Koide

*Photon Factory, IMSS, High Energy Accelerator Research Organization,
Tsukuba, Ibaraki 305-0801, Japan*

A. Tanaka

*Department of Quantum Matter, ADSM, Hiroshima University,
Higashi-Hiroshima 739-8530, Japan*

D. Karmakar

*Technical Physics Division, Bhabha Atomic Research Center, Mumbai
400085, India*

S. K. Mandal and T. K. Nath

*Department of Physics and Meteorology, Indian Institute of Technology,
Kharagpur 721302, India*

I. Dasgupta

*Department of Solid State Physics Indian Association for the Cultivation of
Science Jadavpur, Kolkata 700 032, India*

Abstract

We report on x-ray absorption spectroscopy (XAS) and x-ray magnetic circular dichroism (XMCD) studies of the paramagnetic (Mn,Co)-co-doped ZnO and ferromagnetic (Fe,Co)-co-doped ZnO nano-particles. Both the surface-sensitive total-electron-yield mode and the bulk-sensitive total-fluorescence-yield mode have been employed to extract the valence and spin states of the surface and inner core regions of the nano-particles. XAS spectra reveal that significant part of the doped Mn and Co atoms are found in the trivalent and tetravalent state in particular in the surface region while majority of Fe atoms are found in the trivalent state both in the inner core region and surface region. The XMCD spectra show that the Fe^{3+} ions in the surface region give rise to the ferromagnetism while both the Co and Mn ions in the surface region show only paramagnetic behaviors. The transition-metal atoms in the inner core region do not show magnetic signals, meaning that they are antiferromagnetically coupled. The present result combined with the previous results on transition-metal-doped ZnO nano-particles and nano-wires suggest that doped holes, probably due to Zn vacancy formation at the surfaces of the nano-particles and nano-wires, rather than doped electrons are involved in the occurrence of ferromagnetism in these systems.

1 Introduction

Various semiconducting oxides such as ZnO [1], TiO₂ [2], and SnO₂[3] in thin film and nano-particle forms are known to exhibit ferromagnetism at room temperature when they are doped with transition-metal atoms. Current interest in such magnetic nano-particle systems is motivated by unique electronic structures and magnetism at the surfaces of the nano-particles which are different from the inner core region. In the nano-particle form, the structural and electronic properties are modified by surface defects such as Zn and O vacancies with broken chemical bonds and charge imbalance, which may mediate or modify exchange coupling between the doped atoms [4]. For example, in the case of (Mn,Co)-co-doped ZnO [ZnO:(Mn,Co)] nano-particles [5], high-valence (3+ and 4+) Mn and Co ions are found to be present, probably due to the formation of Zn vacancies (V_{Zn}) in the surface region. The doped Fe atoms in the ferromagnetic ZnO nano-particles are converted from 2+ to 3+ due to hole doping in the surface regions [4, 6, 14], resulting in the ferromagnetic interaction between the doped Fe atoms. In the case of Co-doped ZnO systems such as (Co,Ga)-co-doped ZnO [7] and Co-doped ZnO nano-particles [8], on the other hand, oxygen vacancies (V_O), which induce electron doping, are reported to be necessary for ferromagnetism. Recently, room-temperature ferromagnetism was reported for (Fe,Co)-co-doped ZnO [ZnO:(Fe,Co)] in thin film [9] and nano-particle forms [10]. From the first-principle calculations, Karmakar *et al.* [10] have indicated that V_{Zn} -mediated double exchange interaction plays important role for ferromagnetism in ZnO:(Fe,Co) nano-particles. Indeed, enhance-

ment of ferromagnetic interaction between transition-metal atoms has been demonstrated in previous first-principles calculations by Gopal and Spaldin [11]. First-principle calculations by Park and Min [12], on the other hand, have suggested the importance of RKKY-type exchange interaction mediated by conduction carriers induced by V_O as the origin of ferromagnetism of ZnO:(Fe,Co). Also, calculations by Ghosh *et al.* [13] have indicated direct exchange interaction mediated by the doped electron carriers at the Fe- V_O -Co defect configuration in the surface region of ZnO:(Fe,Co) nano-wires.

Thus, it has been controversial whether the enhancement of exchange interaction comes from electron doping or hole doping. In this paper, we report on x-ray absorption spectroscopy (XAS) and x-ray magnetic circular dichroism (XMCD) studies of paramagnetic ZnO:(Mn,Co) and ferromagnetic ZnO:(Fe,Co) nano-particles. The valence and spin states of the doped ions and their magnetic interaction have been revealed by XAS and XMCD measurements of the transition-metal core levels. Also, both the surface-sensitive total-electron-yield mode and the bulk-sensitive total-fluorescence-yield mode have been employed to extract the valence and spin states of the surface and inner core regions of the nano-particles separately. The experimental results indicate that doped holes rather than doped electrons are involved in the occurrence of ferromagnetism in these systems.

2 Experimental Methods

Transition-metal-co-doped ZnO nano-particles were synthesized by a low temperature chemical pyrophoric reaction process. We have prepared paramagnetic ZnO:(Mn,Co) nano-particles (Mn=15 %, Co=15%), and ferromag-

netic ZnO:(Fe,Co) nano-particles (Fe=5 %, Co=5%) with $T_C > 300$ K. Details of the sample preparation were described in refs.[10, 14, 15]. Structure characterization was carried out by x-ray diffraction (XRD), selected area electron diffraction (SAED) and transmission electron microscopy (TEM). We have made pellets from calcined powders and then sintered them at a temperature of ~ 570 K for 30 min. The average size of the nano-particles were 7-10 nm [10, 14].

XAS and XMCD measurements of ZnO:(Fe,Co) samples and XAS measurements of ZnO:(Mn,Co) samples were performed at the Dragon Beamline BL-11A of National Synchrotron Radiation Research Center (NSRRC), Taiwan. The spectra were taken both in the total-electron-yield (TEY: probing depth ~ 5 nm) and the total-fluorescence-yield (TFY: probing depth ~ 100 nm) modes, i.e., the TEY and TFY modes are relatively surface- and bulk-sensitive, respectively. The degree of circular polarization of x-rays was $\sim 60\%$. XAS and XMCD measurements of ZnO:(Mn,Co) samples were also made at BL-16A of Photon Factory (KEK-PF). The degree of circular polarization of x-rays was more than $\sim 90\%$. All the measurements were performed at room temperature.

Absorption spectra were analyzed using configuration-interaction (CI) cluster-model calculations. The cluster consisted of a transition-metal ion octahedrally and/or tetrahedrally coordinated by O^{2-} ions. The ground state wave function was expanded in the $\psi = \alpha|d^n\rangle + \beta|d^{n+1}\underline{L}\rangle + \gamma|d^{n+2}\underline{L}^2\rangle$, where \underline{L} denotes an ligand O $2p$ hole. The adjustable parameters of the calculation were the charge-transfer energy Δ , the $d-d$ Coulomb energy U , the $p-d$ transfer integral T , and the crystal field splitting parameters $10Dq$. We

assumed high-spin states for the calculations, and 10Dq was assumed to be less than 1.0 eV.

3 Results and Discussion

Figures 1(a) and 1(b) show the Mn and Co $2p \rightarrow 3d$ XAS spectra of the paramagnetic ZnO:(Mn,Co) nano-particles, respectively, taken both in the TEY and TFY modes. In the figures, we compare the experimental spectra (circles) taken both in the TEY and TFY modes with the cluster-model calculations for the Mn and Co ions with various valence states, tetrahedrally co-ordinated by oxygen atoms [19]. From the line-shape analysis shown in Figs. 1(a) and 1(b), the relative concentrations of Mn^{2+} and Co^{2+} ions estimated using TFY mode are higher than those estimated using TEY mode because the features due to the Mn^{2+} and Co^{2+} states in the TEY mode are weak compared to those in the TFY mode. This indicates that the relative concentrations of Mn^{2+} and Co^{2+} ions are relatively high in the inner core region of the nano-particles and those of the higher valence states of Mn^{3+} , Mn^{4+} , Co^{3+} , and Co^{4+} are relatively high in the surface region.

Figures 2(a) and 2(b) show the Mn and Co $2p \rightarrow 3d$ XAS and XMCD spectra of the paramagnetic ZnO:(Mn,Co) nano-particles, respectively, taken in the TEY mode. We compare the Mn $2p \rightarrow 3d$ XMCD spectra of the ZnO:(Mn,Co) nano-particles with those of $\text{Ca}_{1-x}\text{Mn}_x\text{RuO}$ (CMRO) [16] and $\text{Zn}_{1-x}\text{Mn}_x\text{Se}_2$ [17], and compare the Co $2p \rightarrow 3d$ XMCD spectra of the ZnO:(Mn,Co) nano-particles with that of $\text{Ti}_{1-x}\text{Co}_x\text{O}_2$ [18]. It is likely that Mn $2p \rightarrow 3d$ XMCD spectrum comes from the Mn^{3+} and Mn^{4+} ions because the line shape of XMCD spectrum of ZnO:(Mn,Co) is similar to that of CMRO,

where Mn^{3+} and Mn^{4+} ions coexist. The Co $2p \rightarrow 3d$ XMCD spectral line shape of the $\text{ZnO}:(\text{Mn},\text{Co})$ nano-particles is similar to that of $\text{Ti}_{1-x}\text{Co}_x\text{O}_2$. From the experimental results, we suggest that paramagnetic component of the XMCD signals consists of the Mn^{3+} , Mn^{4+} and Co^{2+} states.

Figures 3(a) and 3(b) show the Fe and Co $2p \rightarrow 3d$ XAS spectra of the ferromagnetic $\text{ZnO}:(\text{Fe},\text{Co})$ nano-particles, respectively. In the figures, we compare the experimental spectra (circles) taken both in the TEY and TFY modes with the cluster-model calculations for the Fe and Co ions with various valence states, tetrahedrally or octahedrally co-ordinated by oxygen atoms [19]. In the transition-metal-doped ZnO nano-particles, the valence and the co-ordination of the doped atoms will be $2+(T_d)$ if no vacancies are created, or often become $3+(T_d)$ or $3+(O_h)$ due to the vacancy formation in the surfaces [4, 6]. We therefore calculated spectra for the $2+(T_d)$, $3+(T_d)$, and $3+(O_h)$ states of the Fe and Co ions. Here, O_h is an interstitial site of the Wurzite-type ZnO lattice. From the line-shape analysis shown in Fig. 3(a), one notices that the Fe ions in the surface region are mostly $\text{Fe}^{3+}(O_h)$ with a small amount of $\text{Fe}^{2+}(T_d)$. In the experimental XAS spectra taken in the TFY mode, the dip structure at 710 eV is shallower, that is, the $\text{Fe}^{2+}(T_d)$ component increases in the inner core region, suggesting that $\text{Fe}^{3+}(O_h)$ ions mainly come from the surfaces. From the Co $2p \rightarrow 3d$ XAS spectra, it is likely that the doped Co atoms in the surface region are $\text{Co}^{2+}(T_d)$, $\text{Co}^{3+}(T_d)$ and $\text{Co}^{3+}(O_h)$. On the other hand, the Co atoms in the inner core region appear to be largely in the $\text{Co}^{2+}(T_d)$ state.

Figures 4(a) and 4(b) show the Fe $2p \rightarrow 3d$ XAS and XMCD spectra of the ferromagnetic $\text{ZnO}:(\text{Fe},\text{Co})$ nano-particles, respectively, taken at $H=1$

T. The Fe $2p \rightarrow 3d$ XMCD intensity taken in the TEY mode was finite, while the XMCD spectrum taken in the TFY mode showed low intensity and not clear observed. This indicates that the Fe ions in the surface region but not in the inner core region are magnetically active. Also, one notices that XMCD signals at the Fe L_2 absorption edge are very weak, suggesting that a large orbital magnetic moment (M_{orb}) of the Fe ion, probably due to a mixture of Fe^{2+} component. In the nano-particle form, which has a relatively large surface area, the spin-orbit coupling and magnetic anisotropy may be enhanced due to surface effects. Indeed, this large M_{orb} has been observed for ZnO:Fe nano-particles [6]. Figures 4(c) shows the Fe $2p \rightarrow 3d$ XMCD spectra taken in the TEY mode at various magnetic fields. In Fig. 4(d), the XMCD intensities due to $Fe^{3+}(O_h)$ and $Fe^{2+}(T_d)$ are plotted as a function of magnetic field. The intensity due to $Fe^{3+}(O_h)$ increases with magnetic field but persists at low fields down to $H=0.2$ T, while the XMCD intensity due to $Fe^{2+}(T_d)$ remains unchanged with magnetic field. These results indicate that $Fe^{3+}(O_h)$ contributes to both the ferromagnetism and paramagnetism and that $Fe^{2+}(T_d)$ contributes only to the ferromagnetism.

Figures 5(a) and 5(b) show the Co $2p \rightarrow 3d$ XAS and XMCD spectra of the ferromagnetic ZnO:(Fe,Co) nano-particles, respectively, taken at $H=1$ T. The Co $2p \rightarrow 3d$ XMCD intensity taken in the TEY mode was finite, while the XMCD intensity taken in the TFY mode did not show finite intensity. This suggests that the Co ions in the surface region are magnetically active as in the case of Fe. One can see that the Co $2p \rightarrow 3d$ XMCD spectrum, taken in the TEY mode, comes from the $Co^{2+}(T_d)$ and $Co^{3+}(T_d)$ ions. Figures 5(c) shows the Co $2p \rightarrow 3d$ XMCD spectra taken at various magnetic fields, and Fig.

5(d) shown the Co $2p \rightarrow 3d$ XMCD intensity as a function of magnetic field. This increases with magnetic field, indicating that the ionic Co atoms in the surface region is paramagnetic and that the ferromagnetic component of the Co ions is negligibly small. The negligibly weak XMCD signals in the spectra recorded in the TFY mode indicate that the Co ions in the inner core region is antiferromagnetically coupled, We thus conclude that the ferromagnetism of the ZnO:(Fe,Co) nano-particles comes only from the Fe ions in the surface region.

It should be noted that the Fe $2p \rightarrow 3d$ XMCD spectra of ZnO:(Fe,Co) indicate the spins of $\text{Fe}^{3+}(O_h)$ and $\text{Fe}^{2+}(T_d)$ signals to be in the same directions. Therefore the segregation of ferromagnetic or ferrimagnetic Fe oxides such as ZnFe_2O_4 [20, 21], $\gamma\text{-Fe}_2\text{O}_3$ [22], and Fe_3O_4 [23] can be excluded because in these materials $\text{Fe}^{3+}(T_d)$ and $\text{Fe}^{3+}(O_h)$ are antiferromagnetically coupled [24]. Considering this and from the XRD, SAED and TEM results, we conclude that the ferromagnetism in these nano-particles are intrinsic. A schematic picture of hole-mediated exchange interaction between $\text{Fe}^{3+}(O_h)$ and $\text{Fe}^{2+}(T_d)$ ions is shown in Fig. 6.

4 Conclusion

In summary, we have investigated the electronic structure and magnetism of the paramagnetic (Mn,Co)-co-doped ZnO and ferromagnetic (Fe,Co)-co-doped ZnO nano-particles using $2p \rightarrow 3d$ XAS and XMCD. In the case of ZnO:(Mn,Co) nano-particles, the doped Mn and Co atoms are in a mixed-valence (2+, 3+, and 4+) state and the relative concentrations of the high-valence (3+ and 4+) Mn and Co ions are higher in the surface region than

in the deep core region. Mn and Co $2p \rightarrow 3d$ XMCD results suggest that the paramagnetism comes from the Co^{2+} , Mn^{3+} and Mn^{4+} states. In the case of the $\text{ZnO}:(\text{Fe},\text{Co})$ nano-particles, too, the doped Fe and Co atoms are found to be in a mixed-valence ($2+$ and $3+$) state and the relative concentrations of the Fe^{3+} and Co^{3+} ions are higher in the surface region than in the inner core region. Fe and Co $2p \rightarrow 3d$ XMCD signals due to the ferromagnetic Fe ions and paramagnetic Fe and Co ions were observed in the surface region while no appreciable XMCD signals were observed in the inner core region. From these results, we suggest that the surface region is magnetically active and Fe^{3+} contributes to both the ferromagnetism and paramagnetism, and that Fe^{2+} contributes only to the ferromagnetism. On the other hand, the ionic Co atoms in the surface region is paramagnetic and that the ferromagnetic component of the Co ions is negligibly small. Considering that the Fe^{3+} ions are created due to Zn vacancies, we conclude that the ferromagnetism of $\text{ZnO}:(\text{Fe},\text{Co})$ nano-particles comes from the hole-mediated exchange interaction between $\text{Fe}^{3+}(O_h)$ and $\text{Fe}^{2+}(T_d)$ in the surface region.

5 Acknowledgments

The experiment at PF was approved by the Photon Factory Program Advisory Committee (Proposal No. 2008G010, 2010G187, and 2010S2-001). The work was supported by a Grant-in-Aid for Scientific Research (S22224005) from JSPS, Japan, a Global COE Program the Physical Sciences Frontier”, from MEXT, Japan, an Indo-Japan Joint Research Project Novel Magnetic Oxide Nano-Materials Investigated by Spectroscopy and ab-initio Theories” from JSPS, Japan, and the Quantum Beam Technology Develop-

ment Program Search and Development of Functional Materials Using Fast Polarization-Controlled Soft X-Rays from JST, Japan.

References

- [1] P. Sharma, A. Gupta, K. V. Rao, F. J. Owens, R. Sharma, R. Ahuja, J. M. O. Guillen, B. Johansson, and G. A. Gehring, *Nature Mater.* **2**, 673 (2003).
- [2] T. Yamasaki, T. Fukumura, Y. Yamada, M. Nakano, K. Ueno, T. Makino, M. Kawasaki, *Appl. Phys. Lett.* **94**, 102515 (2009).
- [3] H. Wang, Y. Yan, X. Du, X. Liu, K. Li and H. Jin, *J. Appl. Phys.* **107**, 103923 (2010).
- [4] N. Ganguli, I. Dasgupta and B. Sanyal, *Appl. Phys. Lett.* **94**, 192503 (2009).
- [5] T. Kataoka, Y. Yamazaki, Y. Sakamoto, A. Fujimori, F.-H. Chang, H.-J. Lin, D. J. Huang, C. T. Chen, A. Tanaka, S. K. Mandal, T. K. Nath, D. Karmakar and I. Dasgupta *Appl. Phys. Lett.* **96**, 252502 (2010).
- [6] T. Kataoka, M. Kobayashi, Y. Sakamoto, G.S. Song, A. Fujimori, F.H. Chang, H.J. Lin, D.J. Huang, C.T. Chen, T. Ohkochi, Y. Takeda, T. Okane, Y. Saitoh, H. Yamagami, S.K. Mandal, T.K. Nath, D. Karmakar, and I. Dasgupta, *J. Appl. Phys.* **107** 033718 (2010).
- [7] Y. He, P. Sharma, K. Biswas, E. Z. Liu, N. Ohtsu, A. Inoue, Y. Inada, M. Nomura, J. S. Tse, S. Yin and J. Z. Jiang, *Phys. Rev. B* **78**, 155202 (2008).

- [8] H. Gu, W. Zhang, Y. Xu and M. Yan, Appl. Phys. Lett. **100**, 202401 (2012).
- [9] Y. M. Cho, W.K. Choo, H. Kim, D. Kim, and Y. Ihm, Appl. Phys. Lett. **80**, 3358 (2002)
- [10] D. Karmakar, T. V. Chandrasekhar Rao, J. V. Yakhmi, A. Yaresko, V. N. Antonov, R. M. Kadam , S. K. Mandal, R. Adhikari, A. K. Das, T. K. Nath, N. Ganguli, I. Dasgupta, and G. P. Das, Phys. Rev. B **81**, 184421 (2010).
- [11] P. Gopal and N. A. Spaldin, Phys. Rev. B **74**, 094418 (2006).
- [12] M. S. Park and B. I. Min, Phys. Rev. B **68**, 224436 (2003).
- [13] S. Ghosh, Q. Wang, G. P. Das, and P. Jena, Phys. Rev. B **81**, 235215 (2010).
- [14] D. Karmakar, S. K. Mandal, R. M. Kadam, P. L. Paulose, A. K. Rajarajan, T. K. Nath, A. K. Das, I. Dasgupta, and G. P. Das, Phys. Rev. B **75**, 144404 (2007).
- [15] S. K. Mandal, A. K. Das, T. K. Nath, D. Karmakar, B. Satpati, J. Appl. Phys. **100**, 104315 (2006).
- [16] K. Terai, K. Yoshii, Y. Takeda, S. I. Fujimori, Y. Saitoh, K. Ohwada, T. Inami, T. Okane, M. Arita, K. Shimada, H. Namatame, M. Taniguchi, K. Kobayashi, M. Kobayashi and A. Fujimori, Phys. Rev. B **77**, 115128 (2008).

- [17] A. Hofmann, C. Graf, C. Boeglin, and E. Rühl, *Chem. Phys. Chem.* **8**, 2008 (2007).
- [18] K. Mamiya, T. Koide, A. Fujimori, H. Tokano, H. Manaka, A. Tanaka, H. Toyosaki, T. Fukumura, and M. Kawasaki, *Appl. Phys. Lett.* **89**, 062506 (2006).
- [19] A. Tanaka and T. Jo, *J. Phys. Soc. Jpn.* **61**, 2669 (1992).
- [20] S. Nakashima, K. Fujita, A. Nakao, K. Tanaka, Y. Shimotsuma, K. Miura and K. Hirao, *Appl. Phys. A*: **94**, 83 (2009).
- [21] M. Hofmann, S. J. Campbell, H. Ehrhardt and R. Feyerherm *J. Mater. Science*, **39**, 5057 (2004).
- [22] S. B.-Profeta, M.-A. Arrio, E. Tronc, N. Menguy, I. Letard, C. Cartier Dit Moulin, M. Nogus, C. Chanac, J.-P. Jolivet, Ph. Sainctavit, *J. Mag. Mag. Mater.*, **288**, 354 (2005).
- [23] R. Cornell and U. Schwertmann, *The Iron Oxides* (Wiley & Sons, New York, 1997).
- [24] M. A. Gilleo, *Phys. Rev.* **109**, 777 (1958).

Figures

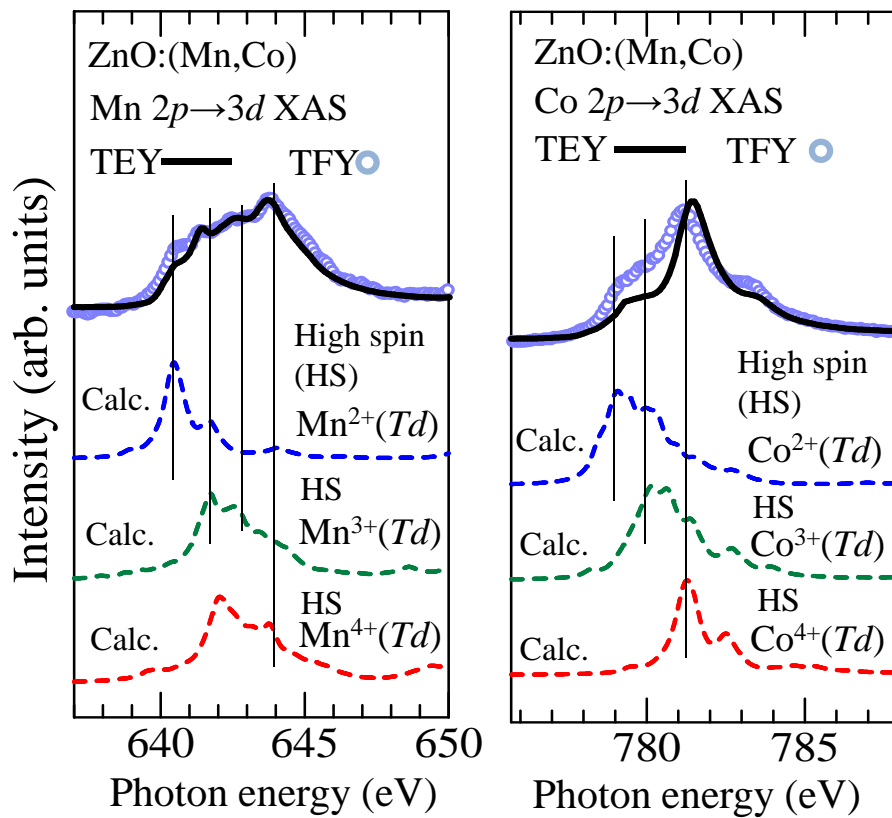


Figure 1: (Color online) Mn and Co $2p \rightarrow 3d$ XAS spectra (circles) of the paramagnetic ZnO:(Mn,Co) nano-particles taken both in the TEY and TFY modes. Theoretical spectra (broken curves) of the Mn and Co ions in the 2+, 3+ and 4+ states calculated using the cluster model are shown.

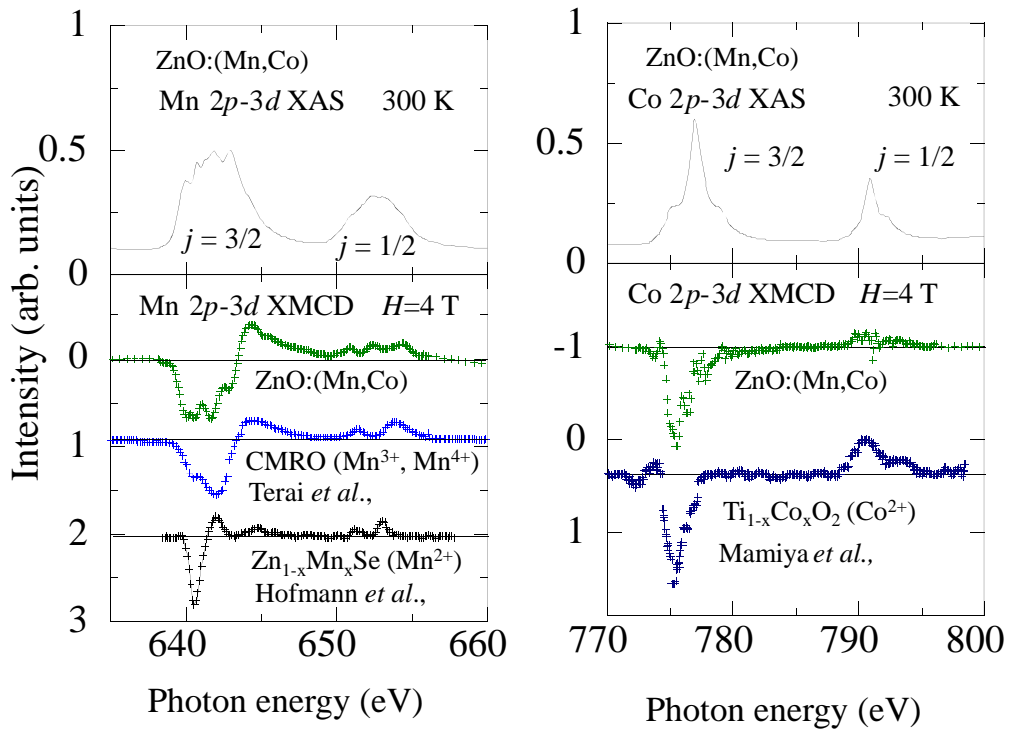


Figure 2: (Color online) Mn and Co $2p \rightarrow 3d$ XAS and XMCD spectra taken in the TEY mode in a magnetic field of $H_T = 4$ T. (a) Mn $2p \rightarrow 3d$ XAS and XMCD spectra of the paramagnetic ZnO:(Mn,Co) nanoparticles and the Mn $2p \rightarrow 3d$ XMCD spectra of Ca_{1-x}Mn_xRuO [16] and Zn_{1-x}Mn_xSe [17]. (b) Co $2p \rightarrow 3d$ XAS and XMCD spectra of the paramagnetic ZnO:(Mn,Co) nano-particles and the Co $2p \rightarrow 3d$ XMCD spectrum of Ti_{1-x}Co_xO₂ [18].

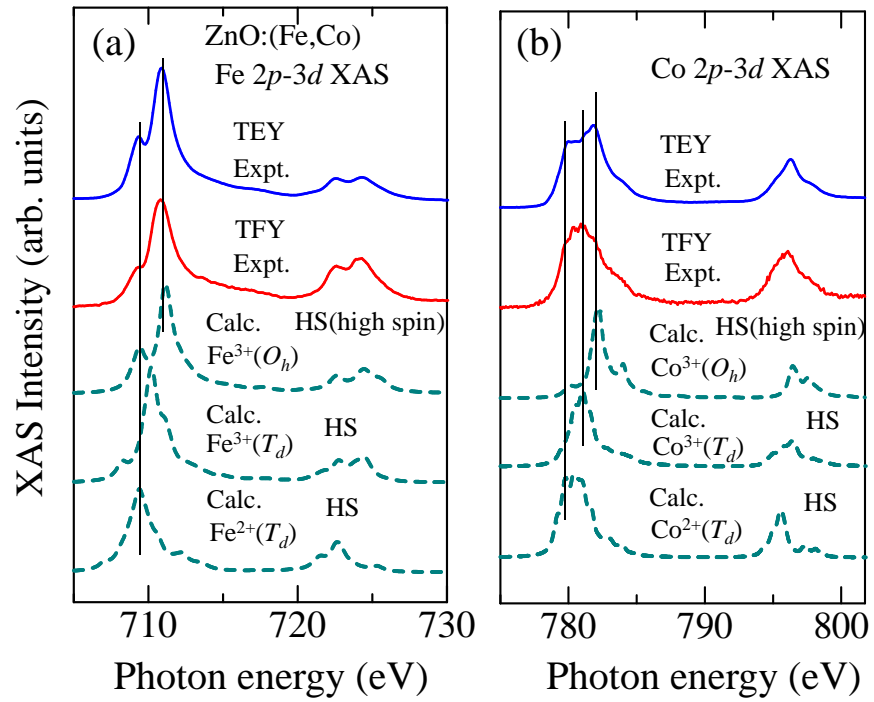


Figure 3: (Color online) Fe (a) and Co (b) $2p \rightarrow 3d$ XAS spectra of the ferromagnetic ZnO:(Fe,Co) nano-particles taken both in the TEY and TFY modes. Theoretical spectra (broken curves) of the Fe and Co ions in the 2+ and 3+ states calculated using the CI cluster-model are shown by dashed curved.

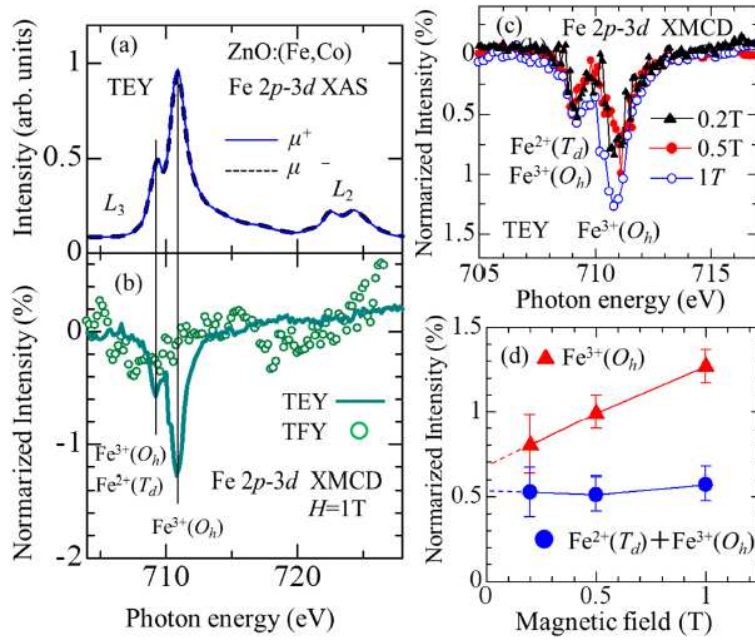


Figure 4: (Color online) Fe $2p \rightarrow 3d$ XAS and XMCD spectra of the ferromagnetic ZnO:(Fe,Co) nano-particles. (a) Fe $2p \rightarrow 3d$ XAS spectra, taken in the TEY mode, in a magnetic field of $H=1$ T. (b) Fe $2p \rightarrow 3d$ XMCD spectra taken both in the TEY and TFY modes. (c) Fe $2p \rightarrow 3d$ XMCD spectra taken in the TEY mode at various magnetic fields. (d) Fe $2p \rightarrow 3d$ XMCD intensity as a function of magnetic field.

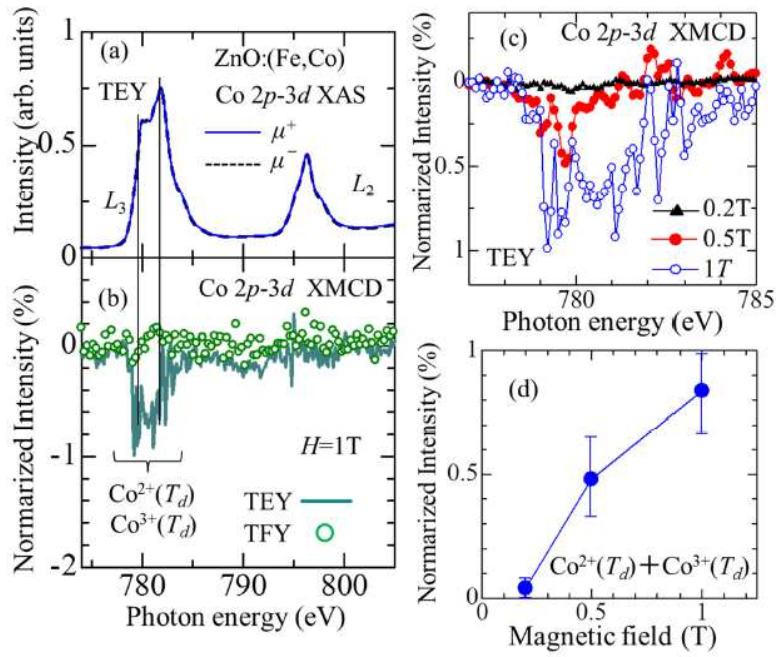


Figure 5: (Color online) Co $2p \rightarrow 3d$ XAS and XMCD spectra of the ferromagnetic ZnO:(Fe,Co) nano-particles. (a) Co $2p \rightarrow 3d$ XAS spectra, taken in the TEY mode, in magnetic fields of $H=1$ T. (b) Co $2p \rightarrow 3d$ XMCD spectra taken both in the TEY and TFY modes. (c) Co $2p \rightarrow 3d$ XMCD spectra taken in the TEY mode at various magnetic fields. (d) Co $2p \rightarrow 3d$ XMCD intensity as a function of magnetic field.

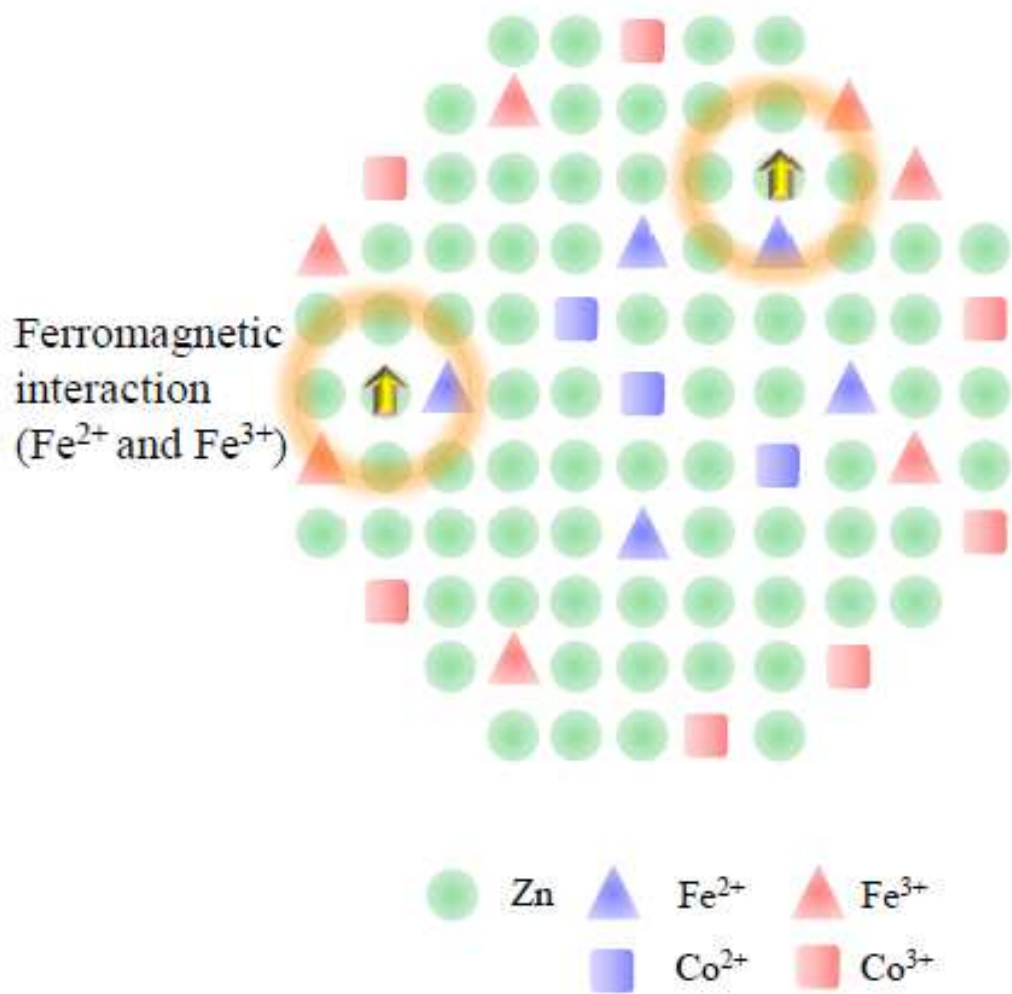


Figure 6: (Color online) A schematic of magnetic interactions in ZnO:(Fe,Co) nano-particles.